NeuroImage 157 (2017) 34–44

Contents lists available at ScienceDirect

NeuroImage

journal homepage: www.elsevier.com/locate/neuroimage

Multifocal tDCS targeting the resting state motor network increases cortical excitability beyond traditional tDCS targeting unilateral motor cortex

D.B. Fischer[a,b,*], P.J. Fried[a], G. Ruffini[c,d], O. Ripolles[d], R. Salvador[d,g], J. Banus[d,h], W.T. Ketchabaw[a], E. Santarnecchi[a], A. Pascual-Leone[a], M.D. Fox[a,e,f,**]

[a] Berenson-Allen Center for Noninvasive Brain Stimulation, Division of Cognitive Neurology, Department of Neurology, Harvard Medical School and Beth Israel Deaconess Medical Center, 330 Brookline Ave, Boston, MA 02215, United States
[b] Harvard Medical School, 25 Shattuck St., Boston, MA 02115, United States
[c] Starlab Barcelona, Avda. Tibidabo 47 bis, 08035 Barcelona, Spain
[d] Neuroelectrics Corporation, 14th Floor, 1 Broadway, Cambridge, MA 02142, United States
[e] Department of Neurology, Harvard Medical School and Massachusetts General Hospital, 175 Cambridge Street – Suite 300, Boston, MA 02114, USA
[f] Athinoula A. Martinos Center for Biomedical Imaging, Massachusetts General Hospital, 149 3th Street, Charlestown, MA 02129, USA
[g] IBEB, Faculdade de Ciências, Universidade de Lisboa, Portugal
[h] Universitat Pompeu Fabra, DTIC, Barcelona, Spain

ARTICLE INFO

Keywords:
FMRI
Resting state
Functional connectivity
Transcranial direct current stimulation
Network stimulation

ABSTRACT

Scientists and clinicians have traditionally targeted single brain regions with stimulation to modulate brain function and disease. However, brain regions do not operate in isolation, but interact with other regions through networks. As such, stimulation of one region may impact and be impacted by other regions in its network. Here we test whether the effects of brain stimulation can be enhanced by simultaneously targeting a region and its network, identified with resting state functional connectivity MRI. Fifteen healthy participants received two types of transcranial direct current stimulation (tDCS): a traditional two-electrode montage targeting a single brain region (left primary motor cortex [M1]) and a novel eight-electrode montage targeting this region and its associated resting state network. As a control, 8 participants also received multifocal tDCS mismatched to this network. Network-targeted tDCS more than doubled the increase in left M1 excitability over time compared to traditional tDCS and the multifocal control. Modeling studies suggest these results are unlikely to be due to tDCS effects on left M1 itself, however it is impossible to completely exclude this possibility. It also remains unclear whether multifocal tDCS targeting a network selectively modulates this network and which regions within the network are most responsible for observed effects. Despite these limitations, network-targeted tDCS appears to be a promising approach for enhancing tDCS effects beyond traditional stimulation targeting a single brain region. Future work is needed to test whether these results extend to other resting state networks and enhance behavioral or therapeutic effects.

Introduction

Scientists and clinicians have traditionally used brain stimulation, both invasive and noninvasive, to target single regions in order to modulate brain function and disease (Nitsche and Paulus, 2000; Nitsche et al., 2003; Fox et al., 2014; Wang et al., 2014; Eldaief et al., 2013; Brunoni et al., 2012). Stimulating primary motor cortex, for example, can increase corticospinal excitability (Nitsche and Paulus, 2000; Horvath et al., 2014) and may improve motor symptoms in stroke and Parkinson's Disease (Horvath et al., 2014; Schlaug et al., 2008; Broeder et al., 2015). However, brain regions do not operate in isolation; they communicate with other regions, through excitatory and inhibitory interactions, in distributed brain networks (Siegel et al., 2015; Yeo et al., 2011; Sporns et al., 2004; Grefkes and Fink, 2014; Grefkes et al., 2008). It is likely that these network-level interactions are influenced by stimulation of a single site, and influence the impact of stimulation at that site (Fox et al., 2014; Wang et al., 2014; Chen et al., 2013; Volz et al., 2015; Nettekoven et al., 2015; Polanía et al.,

Abbreviations: EEG, electroencephalography; FDI, first dorsal interosseus muscle; fMRI, functional magnetic resonance imaging; M1, primary motor cortex; MEP, motor evoked potential; tDCS, transcranial direct current stimulation; TMS, transcranial magnetic stimulation

* Corresponding author at: 45 Green St., Apt B2, Brookline, MA 02446, United States.
** Corresponding author at: 330 Brookline Ave., Kirstein Building KS 151, Boston, MA 02215, United States.
E-mail addresses: d.b.fisch@gmail.com (D.B. Fischer), foxmdphd@gmail.com (M.D. Fox).

http://dx.doi.org/10.1016/j.neuroimage.2017.05.060
Received 12 March 2017; Received in revised form 8 May 2017; Accepted 27 May 2017
Available online 29 May 2017
1053-8119/

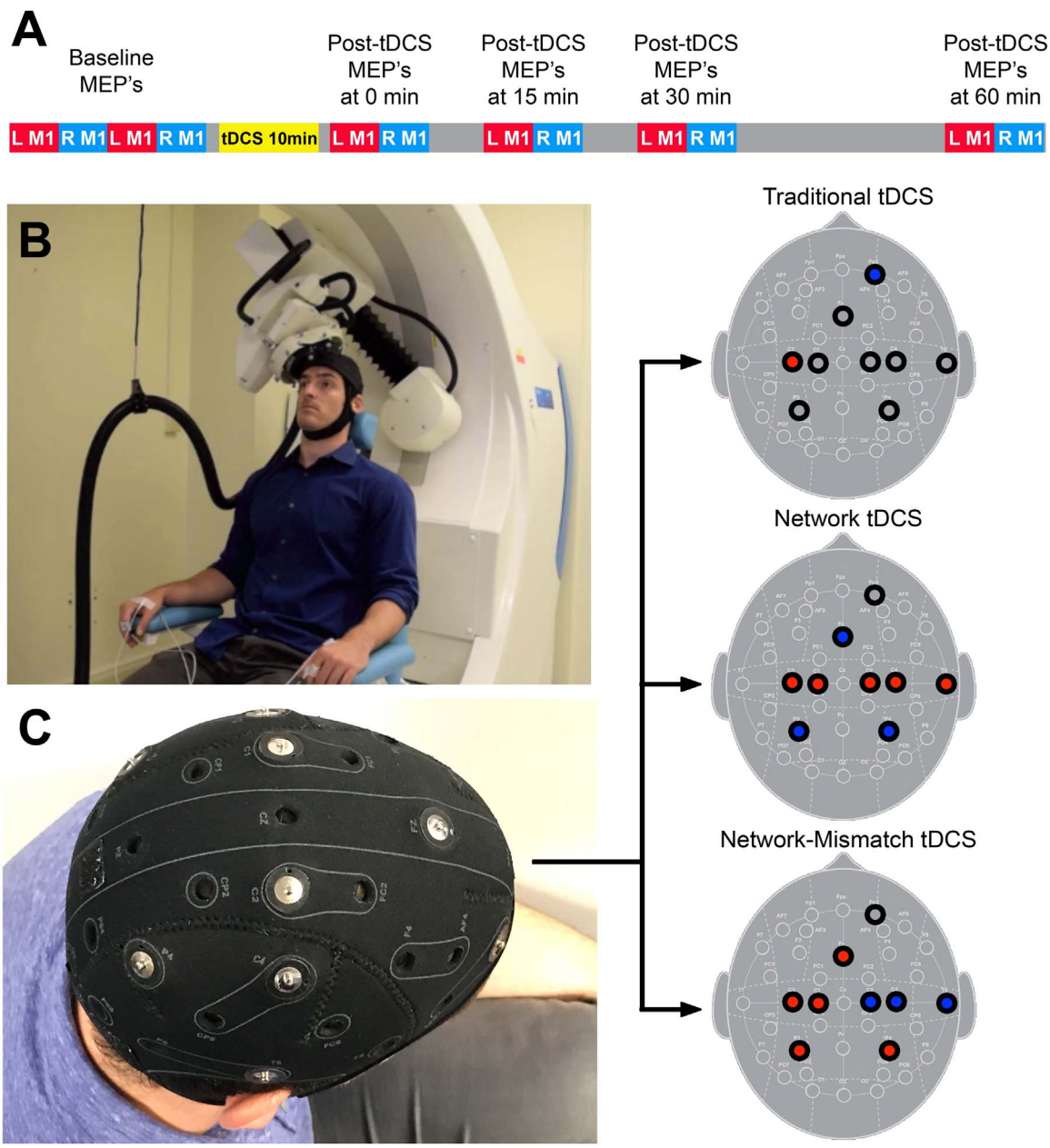

Fig. 1. Experimental design. Motor evoked potentials (MEPs) were assessed at baseline, and after tDCS at regular intervals (A). MEPs were elicited with neuro-navigated robotic TMS to optimize accuracy/precision and minimize bias (B). For all sessions, electrodes were placed in identical locations, with electrical current applied through the electrodes in one of three configurations (C): traditional tDCS (N = 15), network tDCS (N = 15), and network-mismatch tDCS (N = 8). Anodal stimulation is represented in red, cathodal stimulation in blue.

2011). For example, transcranial magnetic stimulation (TMS) administered to brain regions connected to primary motor cortex alters motor cortex excitability and its response to a subsequent TMS pulse (Kujirai et al., 1993; Koch et al., 2007; Pinto and Chen, 2001). If one simultaneously stimulated multiple brain regions connected to primary motor cortex, this could result in a larger effect on motor cortex excitability than stimulating motor cortex alone.

One type of brain stimulation potentially well-suited for targeting a distributed brain network is transcranial direct current stimulation (tDCS) (Ruffini et al., 2014; M.A. Nitsche and Paulus, 2000; Polanía et al., 2011; Polanía et al., 2012; Kuo et al., 2013). Traditionally, tDCS involves two electrodes placed on the scalp surface: a positively charged anode (thought to enhance excitability of underlying cortex) and a negatively charged cathode (thought to suppresses excitability of underlying cortex) (Nitsche et al., 2008). More recently, high-density multi-electrode tDCS arrays have become available (Caparelli-Daquer et al., 2012) and could be used to simultaneously stimulate multiple regions of a distributed brain network (Ruffini et al., 2014). One popular tool for visualizing brain networks is resting state functional connectivity MRI (rs-fcMRI), which identifies functionally associated brain areas through synchronous oscillations of spontaneous brain activity (Yeo et al., 2011; Fox et al., 2005; Fox and Raichle, 2007). Recently, we presented an algorithm for determining the optimal placement and current output of multifocal tDCS electrodes to best target a spatially distributed resting state network (Ruffini et al., 2014). However, this algorithm was based on several assumptions regarding tDCS-induced electric fields, the neurophysiological effect of these electric fields, and the interactions between brain regions within a resting state network (Ruffini et al., 2014). Whether a multifocal tDCS array targeting a brain network results in different neurophysiological effects compared to traditional tDCS targeting a single brain region remains to be tested experimentally.

Here, we conduct the first test of network-targeted stimulation, using multifocal tDCS to simultaneously stimulate left primary motor

cortex (M1) and its associated network, defined using resting state functional connectivity MRI. We selected the motor network for our initial experiments as tDCS effects on motor cortex excitability are reproducible, quantitative, objective, and potentially therapeutically valuable (Broeder et al., 2015; Wu et al., 2009; Horvath et al., 2014). We selected rs-fcMRI as our tool for defining the motor network because the spatial topography of the resting state motor network is highly consistent across individuals (Mueller et al., 2013), rs-fcMRI identifies positive and negative correlations that can guide placement of anodes and cathodes (Fox et al., 2005; Ruffini et al., 2014), and rs-fcMRI can be used to define nearly any brain network (Fox and Raichle, 2007; Yeo et al., 2011), making the current approach potentially useful for targeting networks outside the motor system.

Materials and methods

Participants and study design

Fifteen healthy, right-handed volunteers (11 men, 4 women; ages 33.8 ± 17.8 years) participated in this study. All 15 participants underwent tDCS in two different configurations: traditional tDCS (single anode over left M1 and single cathode over the contralateral supraorbital region) and network tDCS (8 electrodes configured to stimulate multiple regions in the network of left M1). To control for non-specific effects of multifocal tDCS, a subset of these individuals (6 men, 2 women; ages 27.0 ± 15.6 years) additionally underwent network-mismatch tDCS (8 electrodes configured to excite left M1 but suppress remaining regions of the motor network). Only a subset of participants received network-mismatch tDCS because this control condition was added after many participants had already completed the experiment and we wished to counterbalance session order. Each

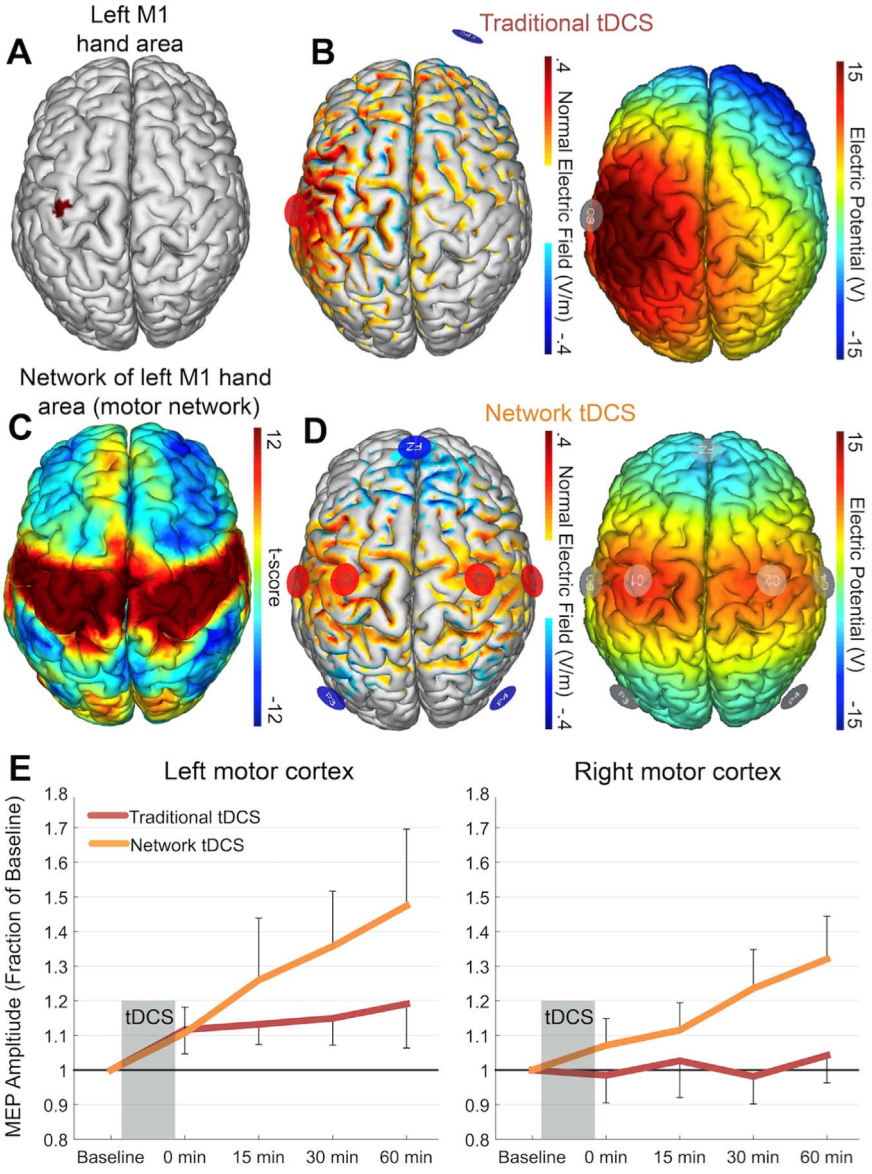

Fig. 2. Traditional versus network tDCS. The hand area of left M1 (A) was targeted by traditional tDCS (B). The left M1 hand area and regions functionally connected to the left M1 hand area (positive correlations in red, negative correlations in blue), constituting the motor network (C), were targeted by network tDCS (D). For both traditional tDCS (B) and network tDCS (**D**), the electrode montage (anodes in red, cathodes in blue), normal / perpendicular component of the electric field (entering cortex in red, exiting cortex in blue), and electric potential are displayed. The electric potential shows the direction in which current will flow (from positive to negative), regardless of particular neuroanatomy. Both conditions shared identical electrode placements, differing only in which electrodes injected current. Network tDCS increased motor excitability compared to traditional tDCS (N = 15) (E). Data are normalized to baseline; for un-normalized data see Fig. S3. Error bars represent standard error of the mean.

session was held on separate days at least 48 h apart. Session order was counter-balanced between participants, including those that received all three stimulation conditions. Each session consisted of a baseline measurement of motor excitability, application of tDCS, and reassessment of motor excitability at regular intervals (Fig. 1). We screened participants for adverse effects of brain stimulation at the start and end of each session. This study was approved by the Beth Israel Deaconess Medical Center Institutional Review Board, and written informed consent was obtained from all participants.

tDCS intervention

In each session, we applied traditional tDCS, network tDCS or network-mismatch tDCS (see montage details below). For all conditions, we delivered tDCS through the Starstim tDCS system (Neuroelectrics, Barcelona, Spain), using 3.14 cm^2 Ag/AgCl gelled electrodes placed into holes of a neoprene cap corresponding to the international 10/10 EEG system, with the central Cz position aligned to the vertex of the head. For all three conditions, we placed electrodes at C1, C2, C3, C4, Fz, P3, P4, T8 and Fp2, although only a subset of these electrodes was used in any one stimulation condition. As such, the cap, gel and electrode placement were identical for all conditions; only the amount of current delivered through each electrode varied. Current was delivered through each electrode via a wireless neurostimulator. For all conditions, tDCS was applied for 10 min, preceded by a 30 s ramp up period and followed by a 30 s ramp down period. Mild tingling, warmth and/or itching were experienced in all conditions.

Traditional tDCS montage

For traditional tDCS, we delivered a total of 2 mA: 2 mA through C3 (the left M1 anode) and −2 mA through Fp2 (the contralateral supraorbital cathode) (Fig. 2B, Fig. S1). We intentionally placed electrodes at standard EEG electrode positions (e.g. C3) instead of individualized positions (e.g. over the motor hotspot), for three reasons. First, this C3-FP2 montage has been used in prior studies to target left M1 (Hanley et al., 2015; Noetscher et al., 2014; Laakso et al., 2015). Second, standardized positioning facilitates modeling of the associated electric fields (Miranda et al., 2013) and thus our optimization algorithm for matching a tDCS configuration to a functional connectivity map (Ruffini et al., 2014). Finally, our goal was to test a generalizable approach to network-targeted stimulation that could potentially be applied to any cortical network, and individualized hotspots are difficult to identify outside of the motor system.

Network tDCS montage. Generating our network tDCS montage consisted of two main steps: 1) identifying the left M1 resting state functional connectivity (rs-fcMRI) map and 2) finding an electrode montage that best matches this network map.

First, we used rs-fcMRI to identify the brain network associated with the left M1 hand area. To do so, we defined a region of interest (ROI) in the left M1 hand area: we used a 6 mm radius sphere based on ROI sizes in prior rs-fcMRI experiments (Fox et al., 2005), and centered the sphere on Montreal Neurological Institute (MNI) coordinates from a prior study of fMRI activation for right hand movements (x=−41, y=−20, z=62; Fig. 2A) (Buckner et al., 2011). We then used this left M1 ROI as a "seed region" to generate a rs-fcMRI map, using an existing rs-fcMRI dataset from 98 healthy, right handed individuals (48 males, ages 22 ± 3.2 years). Details of this dataset and its associated processing have been reported previously (Fox et al., 2012a). Briefly, subjects were instructed to rest quietly in an MRI scanner while spontaneous fluctuations in brain activity were measured. Rs-fcMRI preprocessing steps included spatial smoothing with a 6 mm full-width at half-maximum Gaussian kernel, temporal filtering (0.009–0.08 Hz) and the removal of the following variables by regression: standard six movement parameters, mean whole brain signal, mean brain signal within the lateral ventricles, and the mean signal within a deep white matter ROI. The first temporal derivatives of these regressors were included within the linear model to account for time-shifted versions of spurious variance. Seed-based functional connectivity analysis was performed by extracting spontaneous fluctuations in fMRI activity from the left M1 hand ROI, then computing the Pearson's correlation between this extracted time course and the time course of all other brain voxels. Results were combined across the 98 subjects by converting r values to Fisher z values and performing a random effects analysis (Student's T-test).

The result of this analysis is a map of resting state functional connectivity with the left M1 hand region. The map includes positive correlations over the bilateral primary motor cortex, as reported previously (Yeo et al., 2011; Biswal et al., 1995; Fox and Raichle, 2007), and negative correlations over the prefrontal and parietal cortices (Fig. 2C). The functional significance of negatively correlated brain regions remains a matter of debate (Fox et al., 2009; Murphy et al., 2009), but may reflect brain regions with opposing functions (Fox et al., 2005). Peak coordinates in this rs-fcMRI map were identified using an automated peak search algorithm with a t score threshold of > 4.25 or $< -0.4.25$ (Table S1).

Based on this left M1 rs-fcMRI map, we then used an algorithm (Ruffini et al., 2014) to identify an 8 electrode configuration (based on the 10/10 EEG system) that would produce an electric field optimally matched to this network map (StimWeaver, Neuroelectrics). The details of this algorithm and the finite element model upon which it is based have been published previously (Ruffini et al., 2014; Miranda et al., 2013). Briefly, MRI data from the publically available *Colin27* brain was segmented into 5 different tissues (scalp, skull, cerebrospinal fluid, grey matter and white matter; Fig. S2) using freeware tools (Freesurfer, www.freesurfer.net; ITK-Snap, http://www.itksnap.org/; and SPM 8, http://www.fil.ion.ucl.ac.uk/spm/ with the toolbox MARS, http://neuralengr.com/mars/). The segmentation masks were processed for continuity and smoothed using scripts written in Matlab (www.mathworks.com). The electrodes were modeled as cylinders with a radius of 1 cm and a thickness of 3 mm, representing the conductive gel beneath the electrode cap. A volume FE mesh with ~4.8 million tetrahedral second order elements was created using Iso2Mesh (http://iso2mesh.sourceforge.net/), a Matlab toolbox. The mesh was imported into Comsol (www.comsol.com) where the E-field calculations were performed. All tissues were considered homogeneous and isotropic.

A genetic algorithm was then used to identify the location of electrodes within the 10-10 EEG grid system, and the current to administer through each electrode, to best match the spatial topography of the rs-fcMRI motor network (Ruffini et al., 2014). This algorithm matched the components of the electric field entering the cortex at a normal (i.e., perpendicular) angle (thought to be excitatory) to positive correlations in the motor network map, and components of the electric field exiting the cortex at a normal angle (thought to be inhibitory) to the negative correlations. The ideal solution was the one that minimized error relative to no intervention (ERNI), a goodness of fit measure (Ruffini et al., 2014). The tDCS algorithm was constrained by safety parameters, in which the total injected current could not exceed 4 mA, and no more than 2 mA could be injected per electrode, consistent with the safety limits of the Starstim device. The algorithm identified the optimal electrode configuration and amperage to be: 872 uA from C1, 888 uA from C2, 1135 uA from C3, 922 uA from C4, −1843 uA from Fz, −1121uA from P3, −1036uA from P4, and 183uA from T8 (4 mA total; Fig. 2D).

Network-mismatch tDCS montage. As a control multifocal stimulation condition, network-mismatch tDCS was configured to keep left M1 stimulation similar to or higher than that of network tDCS, while opposing the remaining motor network. The network-

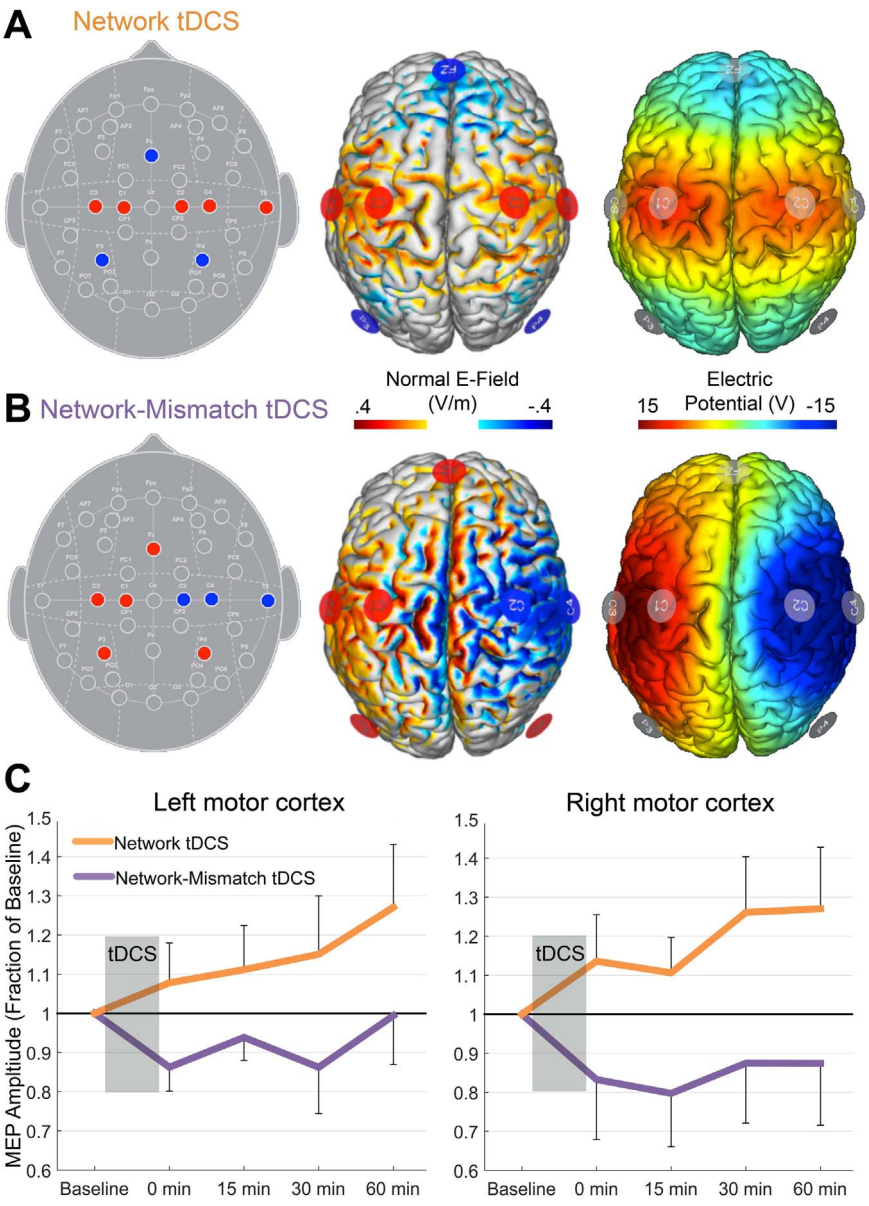

Fig. 3. Network versus network-mismatch tDCS. The electrode configuration and electric potentials of network tDCS (**A**) and network-mismatch tDCS (**B**), with anodes in red and cathodes in blue. Both conditions shared identical electrode placements, differing only in injected current. Network tDCS increased motor excitability, whereas network-mismatch tDCS did not (n = 8) (**C**). Data are normalized to baseline; for un-normalized data see Fig. S4. Error bars represent standard error of the mean.

mismatch configuration controlled for the higher total injected current (4 mA) of network tDCS, and for potential multifocal scalp sensations. We maintained the currents at C1 and C3, and for the remaining 6 electrodes, reversed the polarity from that of network tDCS, such that anodes became cathodes (suppressing positively correlated nodes), and cathodes became anodes (exciting negative correlated nodes). To ensure current conservation, we adjusted the currents for these reversed electrodes, maintaining proportions between cathodes and between non-left M1 anodes (i.e., C2, C4 and T8 were proportionately scaled from network tDCS, as were Fz, P3 and P4). Thus, network-mismatch tDCS was delivered as follows: 872 uA from C1, −1782 uA from C2, 1135 uA from C3, −1851uA from C4, 919 uA from Fz, 559 uA from P3, 515 uA from P4, and −367uA from T8 (4 mA total; Fig. 3B).

We generated all electric field and electric potentials for figures with modeling software (Neuroelectrics Instrument Controller, Neuroelectrics).

Cortical excitability measures

We assessed how each tDCS configuration affected cortical excitability by applying TMS to left and right M1 to elicit muscle contractions from the contralateral hand. The strength of the muscle contraction was recorded as a MEP, the amplitude of which reflects cortical excitability from the targeted M1 region (Bestmann and Krakauer, 2015).

We used a figure-of-8 TMS coil (Model Cool-B65; MagPro X100, MagVenture, Atlanta, Georgia, USA) to find left and right hand motor hotspots, defined as the optimal cortical locations to elicit MEPs from the contralateral first dorsal interosseus muscle (FDI). We held the TMS coil tangential to the head, with the handle rotated approximately 45° away from the midsagittal plane, and delivered single pulses at suprathreshold intensity in ~1 cm intervals. MEPs were measured using surface electromyography, with gelled electrodes positioned over the belly and tendon of the left and right FDI muscle, and recorded at 4 kHz with a band-pass filter of 0.3–1000 Hz, a 5 mV range, a 200 ms timespan of 1024 samples, and a 60 Hz notch and mains filter (Scope,

PowerLab 4/25 T, Ad instruments, Colorado Springs, Colorado, USA). The location and position of the left and right hand motor hotspots were recorded using a neuronavigation system (Localite, Sankt Augustin, Germany) (Santarnecchi et al., 2014). Because most participants did not have their own MRI, a standard MRI brain atlas (MNI152) was used to record the motor hotspots. The use of a standard brain with neuronavigation allows for reproducible positioning of the TMS coil, but does not allow one to relate the hotspot to individual anatomy. Four participants had their own MRI from participation in a prior experiment, and in these cases the participant's own MRI was used for neuronavigation.

After identifying the motor hotspots, we applied the tDCS cap with the stimulation electrodes inserted, and administered electrically conductive gel beneath each electrode with a syringe. We then used a TMS-robot (Axilum, Strasbourg, France) to position the TMS coil over the previously defined left and right stimulation sites at the previously defined orientations (Supplemental Video 1), the first use of such technology to assess tDCS effects. The robotic TMS not only optimized stimulation accuracy and precision (Ginhoux et al., 2013; Richter et al., 2013), which can improve MEP measurements (Toschi et al., 2009), but also eliminated any bias associated with hand-held TMS administration. The TMS-robot held the same TMS coil model used to find the optimal stimulation sites. We adjusted the force sensitivity of the TMS-robot to accommodate the cap and electrodes beneath the coil. TMS was applied over/through the tDCS cap as in prior neuronavigated TMS/tDCS experiments to avoid introducing error into the neuronavigation (Santarnecchi et al., 2014). Specifically, placing and removing the tDCS cap between TMS measurements could displace the subject tracker, resulting in small offsets in the TMS coil position.

Supplementary material related to this article can be found online at doi:10.1016/j.neuroimage.2017.05.060.

Using the robot-administered TMS, resting motor thresholds were computed for both the left and right M1, defined as the minimum TMS intensity required to elicit a peak-to-peak MEP amplitude ≥50 uV in at least 50% of 10 consecutive trials. TMS intensity was increased to 120% of the resting motor threshold, then adjusted to elicit MEPs of 1–1.5 mV (or until maximum stimulator output was reached). Five of our 15 participants required maximum stimulator output at some point during the experiment (3 required max output for both traditional and network tDCS, 1 for network tDCS only, and 1 for traditional tDCS only).

To assess baselines, we used the TMS-robot to deliver 60 single pulses of TMS at the previously determined intensities to each the left and right motor cortices. Baselines were collected in 2 sets of 30, alternating between the left and right hemispheres. All TMS pulses were administered from an automated system that randomly jittered the TMS pulse intervals, such that pulses occurred anywhere between 5 and 10 s apart. For all MEPs, we instructed participants to keep their eyes open and hands relaxed. EMG activity was monitored in real time to ensure muscles were relaxed prior to each TMS assessment. If EMG activity was present, subject's hands were repositioned and relaxation instructions were repeated. We reassessed cortical excitability from both hemispheres immediately after tDCS was complete, 15 min after, 30 min after and 60 min after. At each time point, we delivered 30, jittered, single pulses of TMS to the left, then the right, motor cortices. We recorded the peak-to-peak amplitude of each MEP. In rare cases (< 5% of all blocks), muscle activation was observed between TMS pulses during MEP acquisition. In such cases, the TMS assessment was stopped, all MEPs for that time point were deleted, and 30 MEPs were re-acquired after repeating relaxation instructions. These events almost always occurred during baseline (pre-tDCS) assessment as subjects learned proper hand positioning and relaxation. Participants usually remained seated between measurement periods, but were permitted to stand, walk, and use the bathroom if necessary.

Data analysis

For each participant, tDCS session, and hemisphere, MEPs were averaged at each time point. The first MEP for each time point was excluded, but all other MEPs were included with no post-hoc processing or exclusions. To assess differences between stimulation conditions, considering all time points and both hemispheres, we used a mixed effect linear regression model (SAS Institute Inc., Cary, North Carolina, USA). This approach was selected over the more common analysis of variance (ANOVA) because the linear regression model 1) accounts for the continuity of time (i.e. time points occurring in a specific order) and 2) better accounts for inter-subject variability in baseline MEP (Fitzmaurice et al., 2011). Our linear model included a random intercept for each participant, and fixed effects terms for main effects of baseline MEP, hemisphere, condition (traditional tDCS vs network tDCS vs network-mismatch tDCS), time (minutes from tDCS) and the interactions of time x hemisphere, time x condition, and time x hemisphere x condition. Baseline MEP was included as a fixed effect rather than just another time point so tDCS response would be assessed relative to this baseline. This is similar to MEP normalization often used in tDCS analysis, i.e. computing the ratio between post tDCS and baseline MEPs (M.A. Nitsche and Paulus, 2000; Horvath et al., 2014). However, our approach has the advantage of accounting for variance in tDCS response as a function of baseline MEP, a relationship which has been previously observed (Wiethoff et al., 2014; Tremblay et al., 2016). Including baseline MEP as a fixed effect controls for this variance, allowing us to better identify differences between stimulation conditions. The same model parameters were used to compare traditional tDCS to network tDCS (in all 15 participants), network tDCS to network-mismatch tDCS (in the subset of 8 participants) and traditional tDCS to network-mismatch tDCS (in the subset of 8 participants). All tDCS conditions could not be incorporated simultaneously into a single model, as each contained different numbers of participants. We evaluated significant effects post hoc using stratified analyses, entering data from each hemisphere and each condition separately into the linear model. All statistics were computed using the raw MEP data, which were found to be normally distributed (more so than data normalized to baselines) and thus appropriate for the above statistical analysis. For display purposes, each MEP time point was expressed as a ratio to its respective baseline. Such normalization allows for easier visual comparison between conditions and conforms to convention in the tDCS literature (Lang et al., 2004). Time courses from the raw MEP data are presented as supplemental material.

In a post-hoc analysis, we tested whether differences in muscle activity just prior to each TMS pulse could explain our MEP results. We focused our analysis on the most relevant conditions and time points (traditional tDCS versus network tDCS effects in left M1, baseline versus 60 min post-tDCS). The root-mean-square (RMS) of the EMG for the 50 msec prior to each TMS pulse was computed. Pre-trigger EMG was averaged for the 60 baseline pulses for each subject and the 30 pulses at 60 min post-tDCS. Time points and conditions were compared using paired *t*-tests (two-tailed).

Post-hoc modeling of tDCS and individual differences

To aid in interpretation of results, we performed several modeling analyses. First, we used our *Colin27* head model to estimate the electric field (both total magnitude and normal component) for each of our three tDCS montages. The goodness of fit between our target network (i.e., the rs-fcMRI motor network) and the electric field produced by each of our three tDCS montages was computed using two goodness-of-fit measures as in prior work (Ruffini et al., 2014): the error relative to no intervention (ERNI), and the weighted cross correlation coefficient (WCC). A closer match between the electric field and the target network results in a smaller / more negative ERNI and a WCC closer to 1. To estimate the local effects of our tDCS montages on left M1 itself, we

computed the electric field (total and normal component) within our left M1 ROI, defined by the same 6 mm cortical sphere used to generate the rs-fcMRI motor network.

To ensure that these modeling results, based on a head model from a standard reference brain and group-averaged rs-fcMRI data, generalize to individual participants, we repeated all analyses using individualized MRI data from 4 participants in the present experiment. These four participants completed an MRI scan (GE 3 T HDX scanner) including structural and rs-fcMRI sequences as part of a separate prior experiment. T1-weighted structural images were acquired via a 3D-turbo field echo sequence (TE= 2.9 ms, flip angle=15°, 0.94 × 0.94 × 1 mm voxels). Each subject completed three 6.4 min long resting state fMRI scans (124 volumes, TR=3200 ms, TE=30 ms, flip angle=90°, 3.75 × 3.75 × 3 mm voxels). BOLD imaging employed fat saturation to minimize signal loss and Array Spatial Sensitivity Encoding Technique (ASSET) with acceleration factor 2 to minimize geometric distortion. During the resting state fMRI scans the subjects were asked to lay as still as possible and stare at a fixation cross.

Anatomical MRI data was used to generate four individualized finite element models using the same procedure described above for the *Colin27* brain (Fig. S2) (Ruffini et al., 2014; Miranda et al., 2013). Rs-fcMRI data was processed using the procedures described above, and individualized rs-fcMRI motor networks were identified for these four participants. Finally, individualized left M1 ROIs were defined along the pre-central gyrus based on the anatomical location of the hand knob. Using this individualized data, the electric field intensity within the left M1 ROI, and the fit between the tDCS electric fields and rs-fcMRI motor network, were calculated for each of the four participants.

Results

We compared traditional two-electrode tDCS targeting the left M1 (Fig. 2A, B) to "network" tDCS targeting the left M1 and its associated resting state network (Fig. 2C, D). Network tDCS increased cortical excitability beyond that seen with traditional tDCS (Fig. 2E, Fig. S3). Statistical analysis revealed significant main effects of time (b = 0.019, $t(218)$ = 7.72, $p < 0.0001$), condition (b = −0.22, $t(218)$ = −2.45, $p < 0.05$), and hemisphere (b = −0.27, $t(218)$ = −2.97, $p < 0.01$), with a significant time x condition x hemisphere interaction (b = 0.012, $t(218)$ = 3.68, $p < 0.001$).

Focusing specifically on left M1, network tDCS induced a greater rise in excitability over time (condition x time interaction in left M1, b = −0.02, $t(101)$ = −4.89, $p < 0.0001$), with a trend towards a main effect of condition (b = −0.23, $t(101)$ = −1.83, p = 0.07). At the last time point, one hour after stimulation, the increase in left M1 excitability following network tDCS was more than double the increase following traditional tDCS (47% vs 19% increase) and still rising (Fig. 2E).

In right M1, there was a similar trend towards greater excitability following network tDCS (main effect of condition: b = −0.23, $t(101)$ = −1.80, p = 0.08), but no significant condition x time interaction (b = −0.01, $t(101)$ = −1.28, p = 0.20).

Stratified by condition, there was a main effect of hemisphere in both traditional tDCS (b = −0.27, $t(101)$ = −2.42, $p < 0.05$) and network tDCS (b = −0.29, $t(101)$ = −2.24, $p < 0.05$), whereby both conditions increased left M1 excitability above right M1 excitability. Network tDCS also increased cortical excitability more steeply in left M1 than in right M1 (time x hemisphere interaction in network tDCS, b = −0.01, $t(101)$ = −3.29, $p < 0.01$). A full report of statistical outputs for traditional and network tDCS can be found in Table S2.

In the subset of participants who underwent the control experiment, we compared network tDCS to network-mismatch tDCS. Network-mismatch tDCS was designed to maintain left M1 stimulation and total injected current of network tDCS, but oppose rather than bolster the remaining motor network (Fig. 3A, B). Network-mismatch tDCS did not induce the same elevation in left M1 excitability as network tDCS (Fig. 3C, Fig S4). Statistically, there was a significant main effect of condition, whereby network-mismatch tDCS resulted in cortical excitability below that of network tDCS (b = −0.33, $t(113)$ = −2.96, $p < 0.005$); there were no significant main effects of time or hemisphere, nor were there significant interactions. Considering each hemisphere individually, a main effect of condition was present in right M1 (b = −0.41, $t(52)$ = −2.29, $p < 0.05$), which was expected given the reversed polarity of stimulation there, but also in left M1 (b = −0.29, $t(52)$ = −2.31, $p < 0.05$), where the delivered stimulation was nearly identical between conditions.

Comparing network-mismatch tDCS to traditional tDCS (Fig. S5),

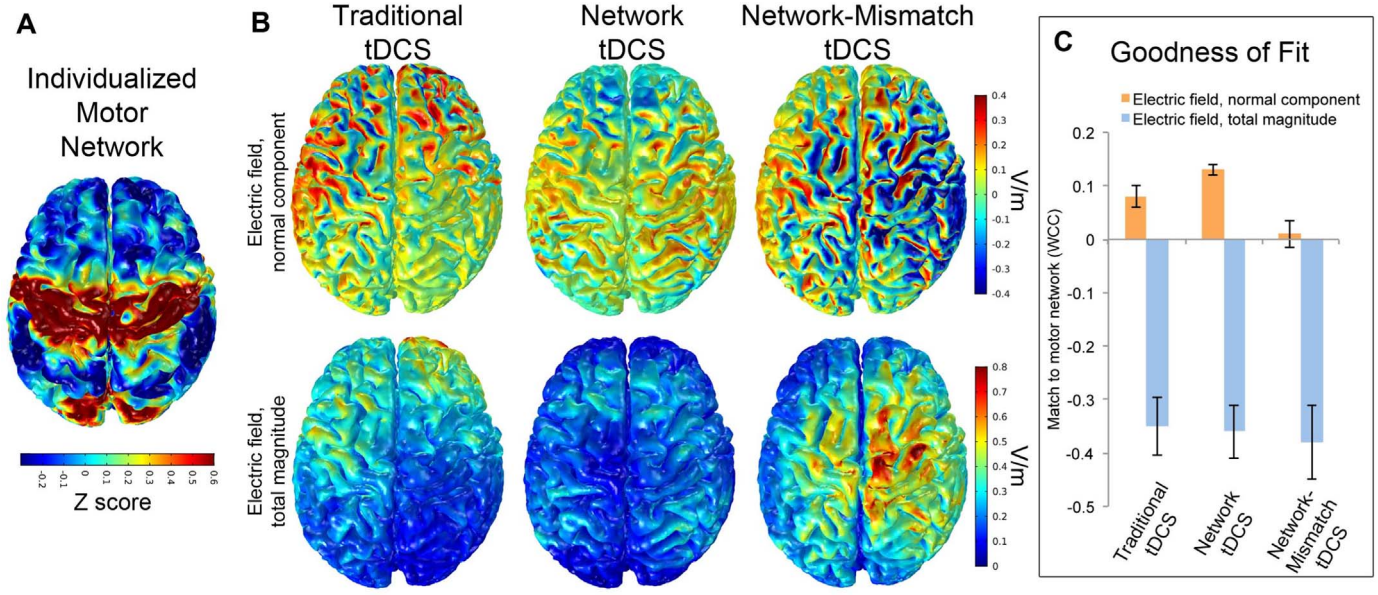

Fig. 4. Individualized motor networks and electric fields. The motor network (A) and modeled electric fields for our three tDCS montages (B) were determined using subject-specific MRI data for a subset of 4 participants. Results from one representative subject are shown here (see Fig. S6, Fig. S7 for other subjects). Both the normal component (top row) and the total magnitude (bottom row) of the modeled electric field are displayed. The fit between each subject's motor network and their individualized electric fields was computed using a weighted cross-correlation coefficient (WCC), averaged across the four participants (**C**). The normal component of the electric field from network tDCS best matches the motor network.

there was a significant main effect of condition, with network-mismatch tDCS suppressing cortical excitability below that of traditional tDCS (b = 0.26, $t(113)$ = 2.27, $p < 0.05$). This effect was significant in left M1 alone (b = 0.30, $t(52)$ = 2.05, $p < 0.05$), with a trend towards significance in the right M1 alone (b = 0.27, $t(52)$ = 1.85, p = 0.07). Thus, network-mismatch tDCS not only failed to elevate left M1 excitability to the same extent as network tDCS, but it effectively suppressed the elevation in left M1 excitability normally induced by traditional tDCS. A full report of statistical outputs for network-mismatch tDCS and its comparisons can be found in Table S3.

There was no carry over of excitability changes between sessions. Specifically, there were no significant differences in baseline excitability in the LM1 (p = 0.89) or RM1 (p = 0.88) between the first and second sessions, even if network tDCS was performed first (LM1, p = 0.88; RM1, p = 0.63). There was no difference in muscle activity prior to the TMS pulses at time points showing the largest MEP effects. Specifically, pre-trigger EMG activity in LM1 was similar at baseline versus 60 min post-tDCS for both the traditional tDCS (0.035 mV vs 0.032 mV, p = 0.56) and network tDCS conditions (0.027 mV vs 0.031 mV, p = 0.35) and was similar at 60 min post-tDCS directly comparing the traditional and network tDCS conditions (0.032 mV vs 0.031 mV, p = 0.90).

To aid in interpretation of the above results, we created finite element head models for four individual participants using the same procedure initially used for the *Colin27* brain (Fig. S2). We used these models to compute the total electric field (Fig. S6) and normal component of the electric field (Fig. S7) for our three tDCS montages. Results for a representative subject are shown (Fig. 4). We estimated the fit of each modeled electric field to the left M1 motor network defined by subject-specific resting state functional connectivity (Fig. 4C, Table S4, S5, S6). We also computed the strength of the modeled electric field within subject-specific left M1 hand knobs (Fig. 5, Fig. S8, Table S7).

The normal component of the electric field from network tDCS provided the best match to the left M1 motor network (compared to other tDCS montages or the total electric field magnitude). In contrast, network tDCS resulted in smaller electric field magnitudes within the left M1 hand knob compared to the other tDCS montages (Fig. 5C). These modeling results were consistent across the five finite element head models (*Colin27* and 4 models from individual subjects; Fig. S8).

Discussion

Here we show that a multifocal tDCS montage designed to stimulate the distributed brain network of left M1, rather than just left M1 alone, resulted in a greater increase in left M1 excitability over time. This was not due to multifocal stimulation per se, as a multifocal array designed to stimulate left M1 but inhibit the remaining network suppressed the excitatory effect of traditional left M1 stimulation. These proof of concept results suggest that the effects of stimulating a target brain region may be augmented by simultaneously targeting other components of that region's network.

Our results following conventional two-electrode tDCS are consistent with prior reports (Nitsche and Paulus, 2001; Horvath et al., 2014). Anodal tDCS with similar parameters produces a ~20% increase in motor excitability that is specific to the stimulated hemisphere and can persist for an hour after stimulation (Nitsche and Paulus, 2001; Horvath et al., 2014). The slightly weaker effects of bifocal tDCS in the current study may be due to the positioning of the anode over C3 rather than the specific motor hotspot or the use of robot-administered TMS, which may reduce bias in MEP assessment. It is worth noting that the current experiment is the first to use robot-administered TMS to assess tDCS effects, but confirms results from prior studies in which the experimenter holding the TMS coil was not always blinded to the tDCS condition (Horvath et al., 2014).

Network tDCS resulted in very different effects on motor excitability compared to traditional tDCS. Although both conditions resulted in a similar increase in left M1 excitability immediately after tDCS, the curves then diverged, with network tDCS causing significantly greater increases in excitability over time. In fact, excitability was still increasing at our last time point, 60 min after stimulation. There was no evidence of persistent effects when participants returned for their next stimulation session (at least 48 h later), however beyond this the duration of network tDCS effects remains unknown.

We are aware of two prior tDCS experiments that found delayed and enhanced increases in motor excitability (Kuo et al., 2013; Nitsche et al., 2004). The first examined the effect of the GABA agonist lorazepam on excitability changes induced by traditional two-electrode tDCS (Nitsche et al., 2004) while the second examined the effect of using a single anode surrounded by a ring of 4 cathodes (Kuo et al., 2013). Both observed slow increases in excitability that peaked 25–

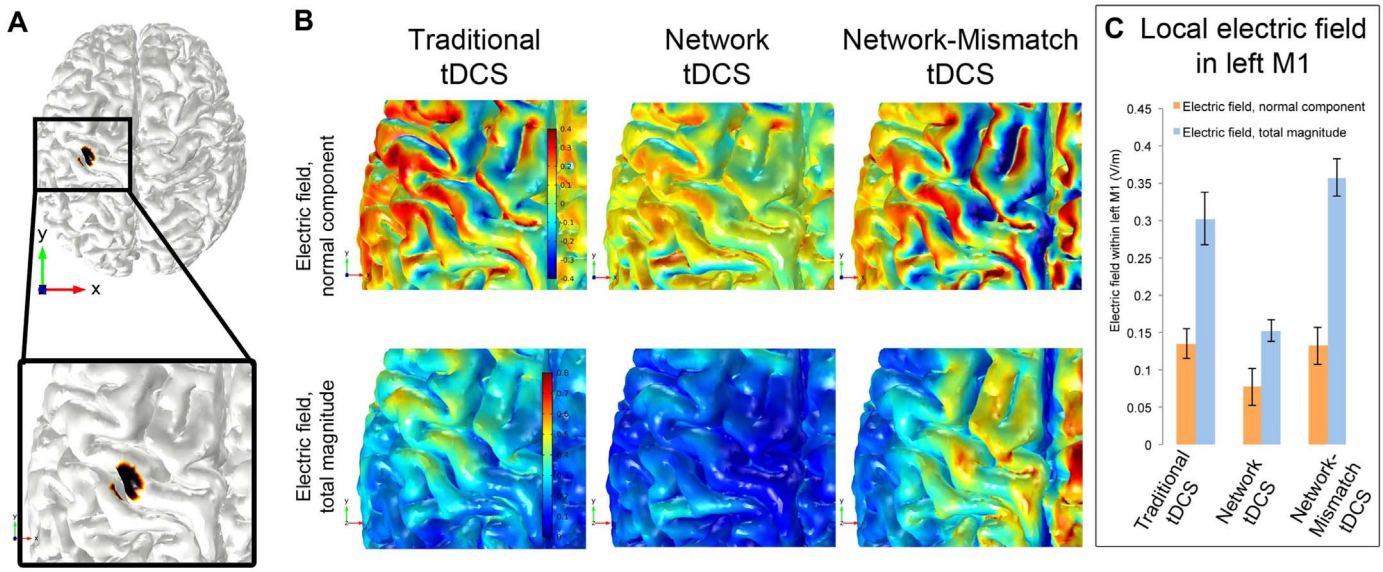

Fig. 5. Electric field strength within the left hand knob does not explain tDCS effects. The left M1 hand knob was identified from the structural MRIs of 4 participants (A); a representative subject is depicted here (see Fig. S8 for other subjects). The normal component (top row) and total magnitude (bottom row) of the electric field was computed for each tDCS montage, displayed with the left M1 magnified (B). The electric field strength within the left M1 hand knob was computed and averaged across the 4 participants (C). Field strength within left M1 was weaker for network tDCS compared to the other 2 montages.

30 min after the stimulation, exceeding the typical duration and magnitude of bifocal tDCS. In both cases, the mechanism was unclear, however one study reasoned that connected brain regions outside M1 must play a role (Nitsche et al., 2004). This interpretation is consistent with the present study, in which remote but connected brain regions were directly targeted with tDCS. To our knowledge, no prior tDCS experiment has observed electrophysiological effects that were still increasing 60 min after the end of stimulation. If replicated in patients, longer lasting tDCS effects could prove valuable for therapeutic applications.

Though network tDCS in this study was designed to enhance left M1 excitability, there was a trend towards simultaneous enhancement of right M1 excitability. This bilateral enhancement runs counter to models of interhemispheric inhibition (Ferbert et al., 1992), and tDCS experiments aimed at improving unilateral motor function by exciting one motor cortex while inhibiting the other (Lindenberg et al., 2010; Lefebvre et al., 2013; Mahmoudi et al., 2011; Vines et al., 2008). While such montages may facilitate stroke recovery, tDCS experiments in healthy subjects using MEP to measure motor excitability are consistent with the present results (O'Shea et al., 2014; Mordillo-Mateos et al., 2012). Specifically, moving the cathode from the supraorbital region to contralateral M1 reduces (rather than enhances) the MEP increase from ipsilateral M1 under the anode (O'Shea et al., 2014; Mordillo-Mateos et al., 2012). Our results are also consistent with the only study to apply anodal stimulation to bilateral M1, which resulted in bilateral improvement in motor function (Gomes-Osman and Field-Fote, 2013). Although further work is needed to understand the relationship between interhemispheric inhibition and tDCS, our results suggest that bilateral increases in cortical excitability are possible. Such effects may prove valuable in diseases where bilateral improvements in function are desired, such as Parkinson's disease (Nitsche et al., 2003; Broeder et al., 2015; Gomes-Osman and Field-Fote, 2013).

Our post-hoc modeling aids in interpretation of our electrophysiological results in two ways. First, the modeling shows that our network tDCS array, designed using a reference brain and group-average functional connectivity, is applicable to individual participants with their own anatomy and connectivity (see Fig. 4). Across these four participants, network tDCS provided the best fit to their individualized resting state motor network compared to the other montages. Whether tDCS arrays customized to each individual's anatomy and functional connectivity results in stronger effects remains unknown. Second, our modeling suggests that differences in left M1 excitability induced by tDCS are unlikely to be due to local effects on left M1 itself (see Fig. 5). Specifically, network tDCS shows weaker electric field strength within the left M1 hand knob compared to the other two montages, yet results in stronger effects on left M1 excitability. While there are inherent limitations to any tDCS modeling approach (Ruffini et al., 2014; Datta et al., 2009; Miniussi et al., 2013) and differences in local M1 effects cannot be completely excluded, tDCS effects on regions outside left M1 seem a more likely explanation.

An unresolved question is which regions outside left M1 are most important for inducing the observed network tDCS effects (e.g. anodes over positive correlations versus cathodes over negative correlations). Our study used a complex algorithm to target the resting state motor network with a multifocal tDCS array, but it is possible that similar results would have been obtained with simple anodal stimulation to bilateral M1 (Gomes-Osman and Field-Fote, 2013). Prior work suggests that tDCS effects are critically dependent on the location of both the anodes and cathodes (Nitsche and Paulus, 2000; O'Shea et al., 2014; Mordillo-Mateos et al., 2012), however the contribution of each electrode to the current results, and whether our algorithm for matching a tDCS montage to a resting state network is optimal for network stimulation, remains unclear.

Another unresolved question is the neurophysiological mechanism underlying the enhanced effects of network tDCS. While TMS and deep brain stimulation induce action potentials that propagate transynaptically to impact connected brain region (Kujirai et al., 1993; Koch et al., 2007; Pinto and Chen, 2001; Hanajima et al., 2004), tDCS is thought to modulate resting membrane potentials, changing the probability of neuronal firing rather than directly inducing action potentials (Nitsche and Paulus, 2000; Bindman et al., 1962). However, neurons are spontaneously active, thus any change in the probability of firing changes the number of spontaneous action potentials (Bindman et al., 1962), which could propagate and impact connected brain regions. Another possibility is that connected brain regions within a network counteract the effects of tDCS to any single region, similar to findings in stroke (Grefkes and Fink, 2014). Simultaneously modulating connected regions could interfere with this compensatory process, enhancing and prolonging tDCS effects. Finally, given recent evidence that single pulses of TMS alone can increase MEP amplitude over time (Pellicciari et al., 2015), it is possible that the different tDCS interventions interacted with the TMS to produce the different excitability changes. Obviously, these mechanistic explanations are speculative and additional work is needed to better understand our observed effects.

The current experiment focused on electrophysiology / MEPs because that is the best-validated measure of tDCS-induced effects (Nitsche and Paulus, 2000; Horvath et al., 2014). Future research may benefit from studying other outcome measures such as brain imaging or behavior. For example, several neuroimaging measures have been used to assess tDCS effects (Polanía et al., 2011; Zheng et al., 2011; Stagg and Nitsche, 2011) and might be useful in assessing the spatial specificity of network tDCS. Similarly, the clinical relevance of network tDCS depends on showing an impact on behavior. Behavioral effects following tDCS are often highly variable (Horvath et al., 2014, 2015; Hashemirad et al., 2016), however the enhanced electrophysiological effects observed here could potentially translate into enhanced behavioral or therapeutic effects. We believe both are possible, as prior work has correlated increases in MEPs with behavior (Garry et al., 2004) and therapeutic benefit (Fregni et al., 2006; Kim et al., 2006).

There are several additional limitations which should be noted. First, while participants were blinded and robot-administered TMS was used to reduce bias, the experimenter administering tDCS was not blinded to the stimulation condition. Second, the adequacy of the participant blinding was not directly assessed, thus participants may have theoretically noticed different scalp sensations between stimulation conditions. However, the two multifocal arrays were matched for total current and electrode size/location, scalp sensations are generally not altered by the location of injected current (Fertonani et al., 2015; Garnett and den Ouden, 2015), and participants were unaware of each condition's hypothesized effect. Third, only 8 of our 15 participants completed the control experiment using network-mismatch tDCS. This number was sufficient to demonstrate significant differences between network tDCS and traditional tDCS, but given this lower sample size effects of network-mismatch tDCS should be interpreted with caution. Finally, the electrode configurations used here were based upon one tDCS modeling approach (Ruffini et al., 2014). While the present results suggest this approach may have predictive value, alternative modeling techniques may result in different, and perhaps superior, solutions (Datta et al., 2009; Miniussi et al., 2013).

Future work is needed to determine whether the enhanced effects of network tDCS on the motor network generalize to other brain networks. It remains unknown whether the stimulation augmentation we observed is idiosyncratic to the motor network, or is attributable to network stimulation more generally. Fortunately, resting state functional connectivity can identify a network associated with any brain region (Fox et al., 2005, 2006; Fox and Raichle, 2007), and the algorithm applied here can identify a multifocal electrode array matched to any brain network (Ruffini et al., 2014). In cases where a single brain region is targeted for neuromodulation – e.g., the dorsolateral prefrontal cortex for depression (Pascual-Leone et al., 1996) – simultaneously targeting other components of that region's network may enhance the neuromodulatory effects. In cases where

functions better localize to networks than to single regions, such as attention (Gitelman et al., 1999; Posner, 2012) and memory (Iidaka et al., 2005), or when treating brain diseases associated with network dysfunction, such as Alzheimer's Disease (Fox et al., 2014; Greicius et al., 2004) and depression (Fox et al., 2014; Broyd et al., 2009; Mayberg, 2009), network-targeted neuromodulation may prove particularly valuable.

In conclusion, our results add to data suggesting that brain connectivity, especially resting state functional connectivity, may be useful for guiding noninvasive brain stimulation (Wang et al., 2014; Chen et al., 2013; Volz et al., 2015; Fox et al., 2014, 2012b). Network tDCS to the motor network appears to enhance the electrophysiological effects of regional stimulation to M1 alone. Further investigation is necessary to determine the mechanism and generalizability of this result. Whether network tDCS will help align neuromodulation with the network-based focus of contemporary neuroscience can be tested in future experiments aimed at modulating cognition, behavior, or disease localizing to brain networks.

Funding

This work was supported by the Howard Hughes Medical Institute, Parkinson's Disease Foundation, Dystonia Medical Research Foundation, NIH/National Institute of Neurological Disorders and Stroke (grant number K23NS083741), Sidney R. Baer Jr. Foundation, NIH (grant numbers R21 NS082870, R01HD069776, R01NS073601, R21 MH099196, R21 NS085491, R21 HD07616), and Harvard Catalyst | The Harvard Clinical and Translational Science Center (NCRR and the NCATS NIH, UL1 RR025758).

Competing Interests

GR is a cofounder, OR is a software development manager, and APL serves on the scientific advisory board of Neuroelectrics, which produces the brain stimulation device and software used in this study. APL serves on the scientific advisory board for Axilum Robotics (which manufactures the TMS robot used in this study), and is listed as an inventor on several issued and pending patents on the real-time integration of TMS with EEG and MRI. MDF is listed as an inventor on pending patents on combining TMS and fMRI. GR, OR, APL and MDF are listed inventors on a filed patent for multifocal tCS.

Appendix A. Supporting information

Supplementary data associated with this article can be found in the online version at doi:10.1016/j.neuroimage.2017.05.060.

References

Bestmann, Sven, Krakauer, John W., 2015. The Uses and Interpretations of the Motor-evoked Potential for Understanding Behaviour. Exp. Brain Res. 233 (3), 679–689.

Bindman, Lynn J., Lippold, O.C.J., Redfearn, J.W.T., 1962. Long-Lasting Changes in the Level of the Electrical Activity of the Cerebral Cortex Produced by Polarizing Currents. Nature 196, 584–585.

Biswal, Bharat B., Yetkin, F.Z., Haughton, V.M., Hyde, J.S., 1995. Functional connectivity in the motor cortex of resting human brain using echo-planar MRI. Magn. Reson. Med.: Off. J. Soc. Magn. Reson. Med. / Soc. Magn. Reson. Med. 34 (4), 537–541.

Broeder, Sanne, Nackaerts, Evelien, Heremans, Elke, Vervoort, Griet, Meesen, Raf, Verheyden, Geert, Nieuwboer, Alice, 2015. Transcranial Direct Current Stimulation in Parkinson's Disease: neurophysiological Mechanisms and Behavioral Effects. Neurosci. Biobehav. Rev. 57, 105–117.

Broyd, Samantha J., Demanuele, Charmaine, Debener, Stefan, Helps, Suzannah K., James, Christopher J., Sonuga-Barke, Edmund J.S., 2009. Default-Mode Brain Dysfunction in Mental Disorders: a Systematic Review. Neurosci. Biobehav. Rev. 33 (3), 279–296.

Brunoni, Andre Russowsky, Ferrucci, Roberta, Fregni, Felipe, Sergio Boggio, Paulo, Priori, Alberto, 2012. Transcranial direct current stimulation for the treatment of major depressive disorder: a summary of preclinical, clinical and translational findings. Progress. Neuro-Psychopharmacol. Biol. Psychiatry 39 (1), 9–16.

Buckner, R.L., Krienen, F.M., Castellanos, A., Diaz, J.C., Yeo, B.T.T., 2011. The organization of the human cerebellum estimated by intrinsic functional Connectivity. J. Neurophysiol. 106 (5), 2322–2345.

Caparelli-Daquer, EgasM., Zimmermann, TrelawnyJ., Mooshagian, Eric, Parra, LucasC., Rice, JustinK., Datta, Abhishek, Bikson, Marom, Wassermann, EricM., 2012. A Pilot Study on Effects of 4×1 High-Definition tDCS on Motor Cortex Excitability. Conference Proceedings: ... Annual International Conference of the IEEE Engineering in Medicine and Biology Society. IEEE Engineering in Medicine and Biology Society. Annual Conference 2012: 735–38.

Chen, Ashley C., Oathes, Desmond J., Chang, Catie, Bradley, Travis, Zhou, Zheng-Wei, Williams, Leanne M., Glover, Gary H., Deisseroth, Karl, Etkin, Amit, 2013. Causal interactions between fronto-parietal central executive and default-mode networks in humans. Proc. Natl. Acad. Sci. 110 (49), 19944–19949.

Datta, Abhishek, Bansal, Varun, Diaz, Julian, Patel, Jinal, Reato, Davide, Bikson, Marom, 2009. Gyri-Precise Head Model of Transcranial Direct Current Stimulation: improved Spatial Focality Using a Ring Electrode versus Conventional Rectangular Pad. Brain Stimul. 2 (4), 201–207.

Eldaief, M.C., Press, D.Z., Pascual-Leone, A., 2013. Trancranial Magnetic stimulation in neurology: a review of established and proespective applications. Neurol. Clin. Pract. 3 (6), 519–526.

Ferbert, A., Priori, A., Rothwell, J.C., Day, B.L., Colebatch, J.G., Marsden, C.D., 1992. Interhemispheric inhibition of the human motor Cortex. J. Physiol. 453, 525–546.

Fertonani, Anna, Ferrari, Clarissa, Miniussi, Carlo, 2015. What Do you feel if i apply transcranial electric stimulation? Safety, sensations and secondary induced Effects. Clin. Neurophysiol. 126 (11), 2181–2188.

Fitzmaurice, Garrett M., Laird, Nan M., Ware, James H., 2011. Applied Longitudinal Analysis 2nd ed. Wiley, Hoboken.

Fox, Michael D., Buckner, Randy L., Liu, Hesheng, Chakravarty, M. Mallar, Lozano, Andres M., Pascual-Leone, Alvaro, 2014. Resting-State Networks Link Invasive and Noninvasive Brain Stimulation across Diverse Psychiatric and Neurological Diseases. Proc. Natl. Acad. Sci. USA 111 (41), E4367–E4375.

Fox, Michael D., Buckner, Randy L., White, Matthew P., Greicius, Michael D., Pascual-Leone, Alvaro, 2012a. Efficacy of Transcranial Magnetic Stimulation Targets for Depression Is Related to Intrinsic Functional Connectivity with the Subgenual Cingulate. Biol. Psychiatry 72 (7), 595–603.

Fox, Michael D., Corbetta, Maurizio, Snyder, Abraham Z., Vincent, Justin L., Raichle, Marcus E., 2006. Spontaneous Neuronal activity distinguishes human dorsal and ventral attention systems. Proc. Natl. Acad. Sci. USA 103 (26), 10046–10051.

Fox, Michael D., Halko, Mark A., Eldaief, Mark C., Pascual-Leone, Alvaro, 2012b. Measuring and Manipulating Brain Connectivity with Resting State Functional Connectivity Magnetic Resonance Imaging (fcMRI) and Transcranial Magnetic Stimulation (TMS)NeuroImage 62, 2232–2243.

Fox, Michael D., Raichle, Marcus E., 2007. Spontaneous fluctuations in brain activity observed with functional magnetic resonance imaging. Nat. Rev. Neurosci. 8 (9), 700–711.

Fox, Michael D., Snyder, Abraham Z., Vincent, Justin L., Corbetta, Maurizio, Van Essen, David C., Raichle, Marcus E., 2005. The human brain is intrinsically organized into dynamic, anticorrelated functional networks. Proc. Natl. Acad. Sci. USA 102 (27), 9673–9678.

Fox, Michael D., Zhang, Dongyang, Snyder, Abraham Z., Raichle, Marcus E., 2009. The global signal and observed anticorrelated resting state brain networks. J. Neurophysiol. 101 (6), 3270–3283.

Fregni, Felipe, Boggio, Paulo S., Santos, Marcelo C., Lima, Moises, Vieira, Adriana L., Rigonatti, Sergio P., Teresa, M., Silva, A., Barbosa, Egberto R., Nitsche, Michael A., Pascual-Leone, Alvaro, 2006. Noninvasive cortical stimulation with transcranial direct current stimulation in Parkinson's disease. Mov. Disord.: Off. J. Mov. Disord. Soc. 21 (10), 1693–1702.

Garnett, Emily O., den Ouden, Dirk-Bart, 2015. Validating a Sham condition for use in high definition transcranial direct current Stimulation. Brain Stimul. 8 (3), 551–554.

Garry, Michael I., Kamen, Gary, Nordstrom, Michael A., 2004. Hemispheric Differences in the relationship between corticomotor excitability changes following a fine-motor task and motor Learning. J. Neurophysiol. 91 (4), 1570–1578.

Ginhoux, R., Renaud, P., Zorn, L., Goffin, L., Bayle, B., Foucher, J., Lamy, J., Armspach, J.P., de Mathelin, M., 2013. A Custom Robot for Transcranial Magnetic Stimulation: First Assessment on Healthy Subjects. Engineering in Medicine and Biology Society (EMBC), 2013 In: Proceedings of the 35th Annual International Conference of the IEEE 2013 (January): 5352–5355.

Gitelman, D.R., Nobre, A.C., Parrish, T.B., LaBar, K.S., Kim, Y.H., Meyer, J.R., Mesulam, M.M., 1999. A large-scale distributed network for covert spatial attention. Brain 122 (6), 1093–1106.

Gomes-Osman, J., Field-Fote, E.C., 2013. Bihemispheric anodal corticomotor stimulation using transcranial direct current stimulation improves bimanual typing task performance. J. Mot. Behav. 45 (4), 361–367.

Grefkes, Christian, Fink, Gereon R., 2014. Connectivity-based approaches in stroke and recovery of function. Lancet Neurol. 13 (2), 206–216.

Grefkes, Christian, Nowak, Dennis A., Eickhoff, Simon B., Dafotakis, Manuel, Küst, Jutta, Karbe, Hans, Fink, Gereon R., 2008. Cortical connectivity after subcortical stroke assessed with functional magnetic resonance imaging. Ann. Neurol. 63 (2), 236–246.

Greicius, Michael D., Srivastava, Gaurav, Reiss, Allan L., Menon, Vinod, 2004. Default-mode network activity distinguishes Alzheimer's disease from healthy aging: evidence from functional MRI. Proc. Natl. Acad. Sci. USA 101 (13), 4637–4642.

Hanajima, R., Ashby, P., Lozano, A.M., Lang, A.E., Chen, R., 2004. Single Pulse Stimulation of the Human Subthalamic Nucleus Facilitates the Motor Cortex at Short Intervals. J. Neurophysiol. 92 (3), 1937–1943.

Hanley, Claire J., Singh, Krish D., McGonigle, David J., 2015. Transcranial modulation of brain oscillatory responses: a concurrent tDCS-MEG investigation. NeuroImage 140,

20–32.
Hashemirad, Fahimeh, Zoghi, Maryam, Fitzgerald, Paul B., Jaberzadeh, Shapour, 2016. The Effect of anodal transcranial direct current stimulation on motor sequence learning in healthy individuals: a systematic review and meta-analysis. Brain Cogn. 102, 1–12.
Horvath, Jared Cooney, Forte, Jason D., Carter, Olivia, 2014. Evidence That transcranial direct current stimulation (tDCS) generates little-to-no reliable neurophysiologic effect beyond MEP amplitude modulation in healthy human subjects: a systematic review. Neuropsychologia 68, 213–236.
Horvath, J.C., Forte, Jason D., Carter, Olivia, 2015. Quantitative Review Finds No Evidence of Cognitive Effects in Healthy Populations from Single-Session Transcranial Direct Current Stimulation (tDCS). Brain Stimul., 1–16.
Iidaka, T., Matsumoto, A., Nogawa, J., Yamamoto, Y., Sadato, N., 2005. Frontoparietal Network Involved in Successful Retrieval from Episodic Memory. Spatial and Temporal Analyses Using fMRI and ERP. Cereb. Cortex 16 (9), 1349–1360.
Kim, Yun Hee, You, Sung H., Ko, Myoung Hwan, Park, Ji. Won, Lee, Kwang Ho, Jang, Sung Ho, Yoo, Woo Kyoung, Hallett, Mark, 2006. Repetitive transcranial magnetic stimulation-induced corticomotor excitability and associated motor skill acquisition in chronic stroke. Stroke 37 (6), 1471–1476.
Koch, Giacomo, Fernandez Del Olmo, Miguel, Cheeran, Binith, Ruge, Diane, Schippling, Sven, Caltagirone, Carlo, Rothwell, John C., 2007. Focal stimulation of the posterior parietal cortex increases the excitability of the ipsilateral motor cortex. J. Neurosci. 27 (25), 6815–6822.
Kujirai, T., Caramia, M.D., Rothwell, J.C., Day, B.L., Thompson, P.D., Ferbert, A., Wroe, S., Asselman, P., Marsden, C.D., 1993. Corticocortical inhibition in human motor cortex. J. Physiol. 471, 501–519.
Kuo, Hsiao-I., Bikson, Marom, Datta, Abhishek, Minhas, Preet, Paulus, Walter, Kuo, Min-Fang, Nitsche, Michael A., 2013. Comparing Cortical Plasticity Induced by Conventional and High-Definition 4×1 Ring tDCS: a Neurophysiological Study. Brain Stimul. 6 (4), 644–648.
Laakso, Ilkka, Tanaka, Satoshi, Koyama, Soichiro, Santis, Valerio De, Hirata, Akimasa, 2015. Inter-Subject Variability in Electric Fields of Motor Cortical tDCS. Brain Stimul. 8 (5), 906–913.
Lang, N., Nitsche, M.A., Paulus, W., Rothwell, J.C., Lemon, R.N., 2004. Effects of transcranial direct current stimulation over the human motor cortex on corticospinal and transcallosal excitability. Exp. Brain Res. 156 (4), 439–443.
Lefebvre, S., Laloux, P., Peeters, A., Desfontaines, P., Jamart, J., Vandermeeren, Y., 2013. Dual-tDCS Enhances Online Motor Skill Learning and Long-Term Retention in Chronic Stroke Patients. Front. Human. Neurosci. 6, 1–17.
Lindenberg, R., Renga, V., Zhu, L.L., Nair, D., Schlaug, G., 2010. Bihemispheric brain stimulation facilitates motor recovery in chronic stroke patients. Neurology 75 (24), 2176–2184.
Mahmoudi, Hooman, Haghighi, Afshin Borhani, Petramfar, Peyman, Jahanshahi, Sepehr, Salehi, Zahra, Fregni, Felipe, 2011. Transcranial direct current stimulation: electrode montage in stroke. Disabil. Rehabil. 33, 1383–1388.
Mayberg, Helen S., 2009. Targeted electrode-based modulation of neural circuits for depression. J. Clin. Investig. 119 (4), 717–725.
Miniussi, Carlo, Harris, Justin A., Ruzzoli, Manuela, 2013. Modelling non-invasive brain stimulation in cognitive neuroscience. Neurosci. Biobehav. Rev. 37 (8), 1702–1712.
Miranda, Pedro Cavaleiro, Mekonnen, Abeye, Salvador, Ricardo, Ruffini, Giulio, 2013. The electric field in the cortex during transcranial current stimulation. NeuroImage 70, 48–58.
Mordillo-Mateos, Laura, Turpin-Fenoll, Laura, Millán-Pascual, Jorge, Núñez-Pérez, Natalia, Panyavin, Ivan, Gómez-Argüelles, José Maria, Botia-Paniagua, Enrique, Foffani, Guglielmo, Lang, Nicolas, Oliviero, Antonio, 2012. Effects of simultaneous bilateral tDCS of the human motor cortex. Brain Stimul. 5 (3), 214–222.
Mueller, Sophia, Wang, Danhong, Fox, Michael D., Yeo, B.T. Thomas, Sepulcre, Jorge, Sabuncu, Mert R., Shafee, Rebecca, Lu, Jie, Liu, Hesheng, 2013. Individual variability in functional connectivity architecture of the human brain. Neuron 77 (3), 586–595.
Murphy, Kevin, Birn, Rasmus M., Handwerker, Daniel A., Jones, Tyler B., Bandettini, Peter A., 2009. The impact of Global signal regression on resting state correlations: are anti-correlated networks introduced? NeuroImage 44 (3), 893–905.
Nettekoven, Charlotte, Volz, Lukas J., Leimbach, Martha, Pool, Eva-Maria, Rehme, Anne K., Eickhoff, Simon B., Fink, Gereon R., Grefkes, Christian, 2015. Inter-individual variability in cortical excitability and motor network connectivity Following multiple blocks of rTMS. NeuroImage 118, 209–218.
Nitsche, M.A., Paulus, W., 2000. Excitability changes induced in the human motor cortex by weak transcranial direct current stimulation. J. Physiol. 527 (3), 633–639.
Nitsche, M.A., Paulus, W., 2001. Sustained excitability elevations induced by transcranial DC motor cortex stimulation in humans. Neurology 57 (10), 1899–1901.
Nitsche, Michael A., Liebetanz, David, Schlitterlau, Anett, Henschke, Undine, Fricke, Kristina, Frommann, Kai, Lang, Nicolas, Henning, Stefan, Paulus, Walter, Tergau, Frithjof, 2004. GABAergic modulation of DC stimulation-induced motor cortex excitability shifts in humans. Eur. J. Neurosci. 19 (10), 2720–2726.
Nitsche, Michael A., Cohen, Leonardo G., Wassermann, Eric M., Priori, Alberto, Lang, Nicolas, Antal, Andrea, Paulus, Walter, et al., 2008. Transcranial direct current stimulation: state of the art 2008. Brain Stimul. 1 (3), 206–223.
Nitsche, Michael A., Schauenburg, Astrid, Lang, Nicolas, Liebetanz, David, Exner, Cornelia, Paulus, Walter, Tergau, Frithjof, 2003. "Facilitation of implicit motor learning by Weak transcranial direct current stimulation of the primary motor cortex in the human. J. Cogn. Neurosci. 15 (1998), 619–626.
Noetscher, Gregory M., Yanamadala, Janakinadh, Makarov, Sergey N., Pascual-Leone, Alvaro, 2014. Comparison of Cephalic and Extracephalic Montages for Transcranial Direct Current Stimulation – a Numerical Study. IEEE Trans. Biomed. Eng. 61 (9), 2488–2498.
O'Shea, Jacinta, Boudrias, Marie H.élène, Stagg, Charlotte Jane, Bachtiar, Velicia, Kischka, Udo, Blicher, Jakob Udby, Johansen-Berg, Heidi, 2014. Predicting behavioural response to TDCS in chronic motor stroke. NeuroImage 85, 924–933.
Pascual-Leone, Alvaro, Rubio, Belen, Pallardó, Federico, Catalá, Maria Dolores, 1996. Rapid-rate transcranial magnetic stimulation of left dorsolateral prefrontal cortex in drug-resistant depression. Lancet 348 (9022), 233–237.
Pellicciari, Maria Concetta, Miniussi, Carlo, Ferrari, Clarissa, Koch, Giacomo, Bortoletto, Marta, 2015. Ongoing cumulative Effects of single TMS pulses on corticospinal excitability: an Intra- and Inter-block investigation. Clin. Neurophysiol. 127 (1), 621–628.
Pinto, A.D., Chen, R., 2001. Suppression of the motor cortex by magnetic stimulation of the cerebellum. Exp. Brain Res. 140 (4), 505–510.
Polanía, Rafael, Nitsche, Michael A., Paulus, Walter, 2011. Modulating functional connectivity patterns and topological functional organization of the human brain with transcranial direct current stimulation. Human. Brain Mapp. 32 (8), 1236–1249.
Polanía, Rafael, Paulus, Walter, Nitsche, Michael A., 2012. Modulating cortico-striatal and thalamo-cortical functional connectivity with transcranial direct current stimulation. Human. Brain Mapp. 33 (10), 2499–2508.
Posner, Michael I., 2012. Imaging attention networks. NeuroImage 61 (2), 450–456.
Richter, Lars, Trillenberg, Peter, Schweikard, Achim, Schlaefer, Alexander, 2013. Stimulus Intensity for Hand Held and Robotic Transcranial Magnetic Stimulation. Brain Stimul. 6 (3), 315–321.
Ruffini, Giulio, Fox, Michael D., Ripolles, Oscar, Miranda, Pedro Cavaleiro, Pascual-Leone, Alvaro, 2014. Optimization of multifocal transcranial current stimulation for weighted cortical pattern targeting from realistic modeling of electric fields. NeuroImage 89, 216–225.
Santarnecchi, Emiliano, Feurra, Matteo, Barneschi, Federico, Acampa, Maurizio, Bianco, Giovanni, Cioncoloni, David, Rossi, Alessandro, Rossi, Simone, 2014. Time Course of Corticospinal Excitability and Autonomic Function Interplay during and Following Monopolar tDCS. Front. Psychiatry 5 (86), 1–11.
Schlaug, G., Renga, V., Nair, D., 2008. Transcranial Direct Current Stimulation in Stroke Recovery. Arch. Neurol. 65 (12), 1571–1576.
Siegel, Markus, Buschman, Timothy J., Miller, Earl K., 2015. Cortical information flow during flexible sensorimotor decisions. Science 348 (6241), 1352–1355.
Sporns, O., Chialvo, D., Kaiser, M., Hilgetag, C., 2004. Organization, development and function of complex brain networks. Trends Cogn. Sci. 8 (9), 418–425.
Stagg, Charlotte J., Nitsche, Michael A., 2011. Physiological basis of transcranial direct current stimulation. Neuroscientist 17 (1), 37–53.
Toschi, Nicola, Welt, Tobias, Guerrisi, Maria, Keck, Martin E., 2009. Transcranial magnetic stimulation in heterogeneous brain tissue: clinical impact on focality, reproducibility and true sham stimulation. J. Psychiatr. Res. 43 (3), 255–264.
Tremblay, Sara, Larochelle-Brunet, F.élix, Lafleur, Louis-Philippe, Mouderrib, Sofia El, Lepage, Jean-François, Théoret, Hugo, 2016. Systematic assessment of duration and intensity of anodal transcranial direct current stimulation on primary motor cortex excitability. Eur. J. Neurosci. 44 (5), 2184–2190.
Vines, Bradley W., Cerruti, Carlo, Schlaug, Gottfried, 2008. Dual-hemisphere tDCS facilitates greater improvements for healthy subjects' non-dominant hand compared to uni-hemisphere stimulation. BMC Neurosci. 9, 103.
Volz, Lukas J., Hamada, Masashi, Rothwell, John C., Grefkes, Christian, 2015. What Makes the Muscle Twitch: Motor System Connectivity and TMS-Induced Activity. Cereb. Cortex 25 (9), 2346–2353.
Wang, Jane X., Rogers, L.M., Gross, E.Z., Ryals, A.J., Dokucu, M.E., Brandstatt, K.L., Hermiller, M.S., Voss, J.L., 2014. Targeted enhancement of cortical-hippocampal brain networks and associative memory. Science 345 (6200), 1054–1057.
Wiethoff, Sarah, Hamada, Masashi, Rothwell, John C., 2014. Variability in response to transcranial direct current stimulation of the motor cortex. Brain Stimul. 7 (3), 468–475. http://dx.doi.org/10.1016/j.brs.2014.02.003.
Wu, Tao, Wang, Liang, Chen, Yi, Zhao, Cheng, Li, Kuncheng, Chan, Piu, 2009. Changes of functional connectivity of the motor network in the resting state in Parkinson's disease. Neurosci. Lett. 460 (1), 6–10.
Yeo, B.T. Thomas, Krienen, Fenna M., Sepulcre, Jorge, Sabuncu, Mert R., Lashkari, Danial, Hollinshead, Marisa, Roffman, Joshua L., et al., 2011. The organization of the human cerebral cortex estimated by Intrinsic functional connectivity. J. Neurophysiol. 106, 1125–1165.
Zheng, Xin, Alsop, David C., Schlaug, Gottfried, 2011. Effects of transcranial direct current stimulation (tDCS) on human regional cerebral blood flow. NeuroImage 58 (1), 26–33.